Influence of Extreme Events and Hydrogeological Properties on the Release Capacity of Store-and-Release Covers in a Semiarid Climate

GEOQuébec 2015
Challenges from North to South
Des défis du Nord au Sud

Bossé B., Bussière B., Maqsoud A. & Benzaazoua M.
Research Institute on Mines and the Environment, UQAT, Rouyn-Noranda, Québec, Canada
Hakkou R.
Faculté des Sciences et Techniques, Université Cadi Ayyad, Marrakech, Morocco

ABSTRACT
The transient unsaturated hydrogeological behaviour of four store-and-release (SR) cover systems made with different fine-grained materials was simulated using the HYDRUS-1D code under extreme rainfall conditions typical of a semiarid climate. Numerical predictions indicated higher release rates for coarser SR materials (0.3 mm/d), whereas finer SR materials (0.03 mm/d) accumulated water above the interface of the cover systems and did not prevent water percolation with the reactive mine wastes under consecutive extreme rainfall events. Coarser SR materials (*i.e.*, silty sands), which recover their full storage capacity more rapidly, proved more suitable to ensure the long-term performance of these systems under natural and extreme climatic conditions. The surface evaporative fluxes, the thickness of the SR layer and the hydrogeological properties of the fine-grained material are the main parameters that affect the release capacity of such cover systems.

RÉSUMÉ
Le comportement hydrogéologique transitoire de quatre systèmes de recouvrement alternatifs constitués de différents matériaux fins a été simulé, en utilisant le code numérique HYDRUS-1D, sous des conditions de précipitations extrêmes typiques d'un climat semi-aride. Les prédictions numériques ont montré que les matériaux plus grossiers ont des taux de libération plus élevés (0.3 mm/j) alors que les matériaux plus fins (0.03 mm/j) ont eu tendance à accumuler l'eau au-dessus de l'interface des systèmes de recouvrement et n'ont pas empêché la percolation avec les résidus miniers réactifs lors d'événements de précipitations extrêmes successifs. Les matériaux plus grossiers (*i.e.*, sables silteux), qui récupèrent plus rapidement leur pleine capacité de stockage, ont montré une meilleure capacité à garantir la performance à long terme de ces systèmes, pour des conditions climatiques naturelles et extrêmes. Le flux évaporatoire en surface, l'épaisseur de la couche et les propriétés hydrogéologiques du matériau à granulométrie fine sont les principaux paramètres qui affectent la capacité de libération de ces systèmes de recouvrement.

1 INTRODUCTION

Store-and-release (SR) cover systems based on soil–atmosphere interactions and capillary barrier effects, also referred to as water balance, evapotranspiration and alternative covers, are increasingly used in arid and semiarid climates to reduce deep water infiltration (percolation) and to control contaminated drainage production from mine wastes disposal areas (*e.g.*, Bossé et al. 2013, 2015a; Zhan et al. 2014). The transient unsaturated hydrogeological behaviour of these systems allows a fine-grained SR material to retain water during wet periods and release it to the atmosphere by evaporation (or evapotranspiration) during dry periods.

To design an SR cover system, numerical modeling studies are commonly performed to determine the influence of the type of material and the thickness of the SR layer on its storage capacity, and to predict long-term hydrogeological performance under normal and extreme climatic conditions (*e.g.*, Morris and Stormont 1998; Khire et al. 2000; Ogorzalek et al. 2008; Bohnhoff et al. 2009). Khire et al. (2000) have shown that increasing the thickness of SR layers made with materials having low saturated hydraulic conductivities (k_{sat}) (*i.e.*, sandy silts, silty sands, silts and clayey sands) increases the storage capacity and reduces percolation. Bossé (2014) has also investigated the influence of the SR layer thickness and showed that an increase of the thickness affects the main water balance components (*i.e.*, water storage, percolation and actual evaporation). However, Khire et al. (2000) and Bossé (2014) also noted that accumulation of water may occur for too-thick SR layers and after significant rainfall events which reduces long term storage capacity.

Using field experimental cells exposed to natural and extreme rainfall conditions, Bossé et al. (2015a) have recently suggested that appropriate hydrogeological properties of fine-grained SR materials may decrease the period of water accumulation in the SR layer by improving the release capacity of the cover system. In other words, the ideal SR material would store water during precipitation events but would release rapidly water to the atmosphere allowing the system to regain its full capacity to manage the next precipitation events (without water accumulation at the bottom of the SR layer). Nevertheless and due to the difficulty in understanding the main mechanisms that control the release process by evaporation (or evapotranspiration), only a few studies have taken into account the natural release capacity of fine-grained materials to design SR cover systems (*e.g.*, Bossé et al. 2015a); the emphasis in the design process is usually on the storage capacity (*e.g.*, Morris and Stormont 1998; Khire et al. 2000; Ogorzalek et al. 2008; Bohnhoff et al. 2009).

This study investigated the influence of the hydrogeological properties of SR materials on their release capacity after extreme rainfall events. First, numerical predictions, obtained with a one-dimensional code that incorporate soil–atmosphere interactions, of four SR covers made with different fine-grained materials were compared. These predictions were performed for extreme rainfall conditions typical of a semiarid climate, which were simulated during the first day. Then, consecutive extreme rainfall events were applied over ten years for identifying which fine-grained materials could cause water percolation due to a lower release capacity. This paper makes an original contribution by evaluating the capacity of different SR materials to manage successive extreme rainfall events. It is inspired from a recent study performed in Morocco where experimental cells were built to test different SR cover systems that aim at controlling acid mine drainage production from an abandoned mine site (Bossé et al. 2015a).

2 MATERIALS AND METHODS

2.1 Main hydrogeological properties

The main physical properties of the four SR materials tested are given in Table 1. Materials particle size distribution were determined using a Malvern Mastersizer laser particle size analyzer (Merkus 2009) and by sieving (ASTM D6913-04 2009). Standards tests (ASTM D4318-10 2010a) for liquid limit (< 50), plastic limit and plasticity index were also performed. According to the Unified Soil Classification System (USCS), the grain-size distributions of the SR materials are typical of silty sand with gravel (SM-G), silty sand (SM), sandy silt (ML) and lean clay with sand (CL), whereas the grain size distribution of the capillary break (CB) material is typical of poorly graded gravel with sand (GP).

Detailed results of the hydrogeological characterization of the SR and CB materials are presented in Bossé (2014) and summarized in Tables 1 and 2. For the SR materials, the saturated hydraulic conductivities (k_{sat}) were measured using a flexible wall permeameter (ASTM D5084-10 2010b). The SR materials have a k_{sat} value ranging from 1.9×10^{-6} to 3.7×10^{-5} cm/s. For the CB material, the k_{sat} value, measured using a rigid-wall permeameter with constant head (ASTM D2434-68 2006), was 5.9 cm/s.

Table 1. Hydrogeotechnical properties of SR cover materials

Classification (USCS)			Particle size distribution					
Material	**Symbol**	**Name**	**Gravel (%)**	**Sand (%)**	**Silt (%)**	**Clay (%)**	**PI**	**k_{sat} (cm/s)**
SR material (1)	**SM-G**	Silty sand with gravel	15.1	48.5	29.3	7.1	0.8	3.7×10^{-5}
SR material (2)	**SM**	Silty sand	1.0	53.1	36.9	9.0	0.8	9.8×10^{-6}
SR material (3)	**ML**	Sandy silt	0.0	40.0	47.5	12.5	0.8	6.0×10^{-6}
SR material (4)	**CL**	Lean clay with sand	0.0	15.5	72.5	12.0	9.4	1.9×10^{-6}
Capillary Break	**GP**	Poorly graded gravel with sand	84.0	15.0	1.0	0.0	NA	5.9×10^{0}

Note: USCS, Unified Soil Classification System (ASTM D2487 2011), gravel (>4.75 mm), sand (4.75–0.075 mm), silt (0.075–0.002 mm), clay (<0.002 mm); PI, plasticity index; k_{sat}, saturated hydraulic conductivity (geometric mean); NA, not applicable.

Table 2. Hydrogeological properties and van Genuchten parameters

Material	**Symbol**	**θ_r**	**θ_s**	**α (kPa^{-1})**	**n**	**m**
SR material (1, 2, 3)	**SM-ML**	0.01	0.43	0.122	1.43	0.301
SR material (4)	**CL**	0.03	0.41	0.151	1.55	0.356
Capillary Break	**GP**	0.01	0.38	0.73	4.94	0.797

Note: θ_r, residual volumetric water content; θ_s, saturated volumetric water content; α, *n*, *m*, van Genuchten (1980) parameters.

The water retention curves (WRCs) were obtained using laboratory instrumented column tests. Figure 1a shows the WRCs of the SR (field data) and the CB (laboratory data) materials fitted with the van Genuchten model (1980; see the fitted equation parameters in Table 2) and Figure 1b shows the hydraulic conductivity functions obtained using the van Genuchten–Mualem (1980) equation. In this specific case and under semiarid and arid climatic conditions, field data were generally closer to the main wetting curves (MWCs – Bossé et al. 2013, 2015a). In addition, under these specific conditions, preliminary non-hysteretic simulations based on measured or predicted MWCs were recently recommended for assessing the performance of SR cover systems and making preliminary predictions of water percolation (Bossé et al. 2015b). For this reason, only the MWCs of the SR materials have been considered in this study. Note that the MWCs of the SR materials 1, 2 and 3 were considered similar (see Table 2).

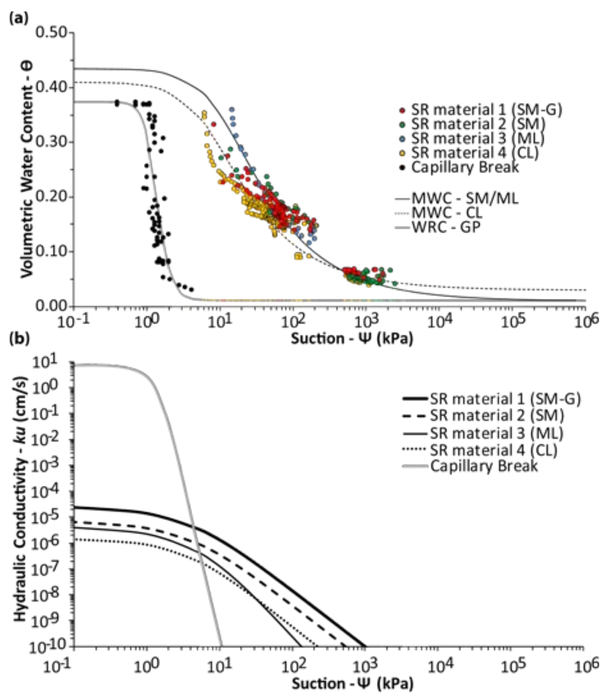

Figure 1. (a) Main water retention curves (WRCs) and (b) hydraulic conductivity functions of the four SR materials and the CB material; MWC, main wetting curve

2.2 Numerical modeling

The HYDRUS-1D code uses Galerkin-type linear finite element schemes to numerically solve the Richards equation (1931), obtained by combining Darcy's law and the conservation of mass equation, for unsaturated water flow (*e.g.*, Šimůnek et al. 2009). Additionally, HYDRUS-1D can simulate soil-atmosphere interactions, hysteresis effects, heat and solute transport, vapor flow and soil extraction by plants. This code was selected because it has been used to assess the performance of engineered cover systems and it is suitable for simulating the near-surface water balance (for more information, see Scanlon et al. 2002). It is important to recall that Bossé et al. (2015b) have previously validated the HYDRUS-1D predictions with field data obtained from similar SR covers exposed to semiarid climatic conditions.

2.2.1 Initial conditions and numerical parameters

In this study, numerical simulations were conducted to predict the hydrogeological behaviour of four SR covers having a total height of 130 cm, and consisting of 100 cm of a fine-grained material overlying 30 cm of coarse-grained material (see section 2.1 for materials' properties).

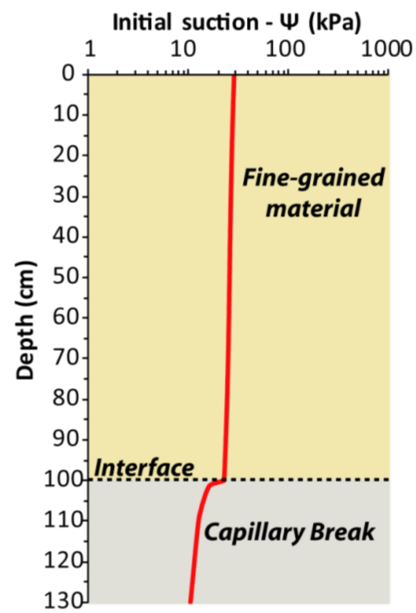

Figure 2. Simulated SR cover configuration and initial suctions used at the beginning of the simulations; Figure 4 shows the initial volumetric water content profiles

This 1D model was discretized into 221 nodes with a nodal spacing of 10 mm. However, an element thickness of 1 mm was strategically used at the top and at the interface of the two materials with opposing textures, where atmospheric interactions and capillary barrier effects could increase numerical difficulties. An initial matric suction profile (Fig. 2) was assigned to each node. Knowing that the MWCs of the fine-grained materials were relatively similar, only one matric suction profile is showed in Figure 2. This profile was obtained using specific boundary conditions, where a significant precipitation was applied (*i.e.*, 155 mm over a period of 24 h) and a drainage period was allowed to obtain a relatively uniform volumetric water content profile.

The temporal discretization applied for the transient analysis consisted of a maximum and minimum time step of 24 and 2.4×10^{-5} h, respectively. Isothermal water flow was simulated and the numerical approach did not consider vapor flow or heat transport.

2.2.2 Boundary conditions

Two main boundary conditions were assigned to the transient simulations at the top and bottom, respectively. The upper boundary condition simulated atmospheric interactions (Fig. 3) and free drainage condition was assigned to the column bottom (*e.g.*, Benson 2007). For the upper condition, only daily potential evaporations computed by HYRDUS-1D using the Penman-Monteith equation were applied (annual potential evaporation of the bare fine-grained material ≈ 1 000 mm). Under natural conditions, knowing that rainfall events (annual rainfall ≈ 250 mm) only affected the surface of the cover systems in the field (mainly the first 10 cm), and the total net infiltration were rapidly released to the atmosphere (see Bossé et al., 2013; 2015b), natural rainfall events were neglected to facilitate numerical convergence. The simulations are a simplified case of the reality but will give a good representation of the release capacity of the tested systems after an extreme rainfall event. The hCritA value, controlling soil–atmosphere interactions in the HYDRUS-1D code, was set at 10 000 kPa (for more information, see Bossé 2014 and Bossé et al., 2015b).

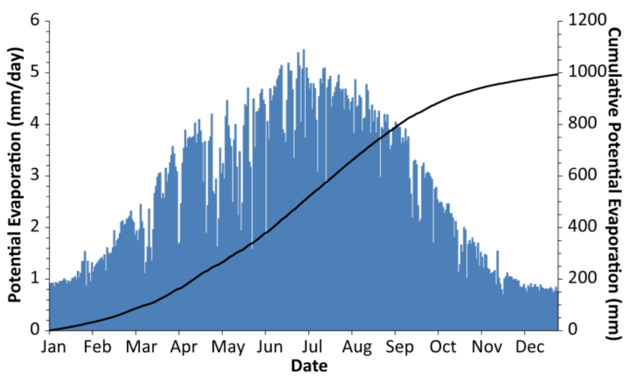

Figure 3. Climatic data (potential evaporation) used for the upper boundary condition

3 RESULTS

The main objective of the first series of numerical analysis was to compare the release capacity of the four tested SR materials. The numerical simulations were performed using HYDRUS-1D and the WRC parameters presented in Table 2. Figures 4 and 5 show predicted volumetric water content (θ) profiles for each SR cover system and the simulated volumetric water content (θ) time trends at the observation point located at 75 cm depth. Figures 6a and 6b show the predicted water storage time trends and the cumulative release rate of the extreme rainfall event (155 mm).

3.1 Volumetric water contents

For each SR cover system (Fig. 4), three profiles are presented: the initial volumetric water content profile (t = 0 day; see Section 2.2), the volumetric water content profile five years after the extreme rainfall simulation (t = 1 825 days = 5 years), and the final volumetric water content profile at the end of the testing period (t = 3 650 days = 10 years). In each case, the CB layer was not affected (no percolation was predicted).

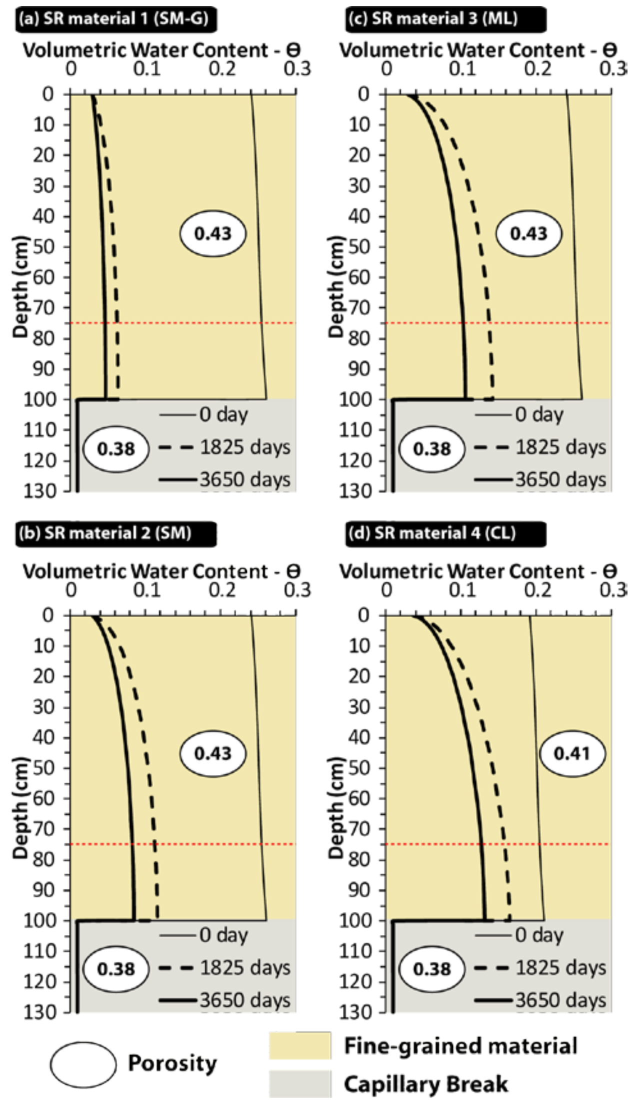

Figure 4. Predicted volumetric water content profiles for the four cover systems made with SR material 1 (a), 2 (b), 3 (c) and 4 (d); porosity is considered equal to the volumetric water content at full saturation (ψ = 0) of each material (Fig. 1) and Figure 5 shows the predicted volumetric water content time trends at 75 cm depth (red dotted lines)

For the tested cover systems, the initial predicted volumetric water contents profiles show θ values ranging from 0.20 to 0.26. The predicted volumetric water contents decreased progressively with time. Although θ values were rapidly close to 0.03 at the surface of the four cover systems, five years after the extreme rainfall event, θ reached 0.06, 0.12, 0.14 and 0.17, respectively, at 100 cm depth for the SR materials 1 (SM-G), 2 (SM), 3 (ML) and 4 (CL). The final volumetric water content profiles (ten years after the extreme rainfall simulation) shows lower values at the top (0 cm) than at the bottom (100 cm) of the SR material: values ranging from 0.03 to 0.05 for the coarser material (SR material 1 – SM-G) and from 0.04 to 0.13 for the finer material (SR material 4 – CL) (Fig. 4a and 4d). At 100 cm depth, θ reached respectively 0.08 and 0.10 for the SR materials 2 (SM) and 3 (ML) (Fig. 4b and 4c). Note that a relatively uniform θ profile close to the residual value is observed only for the coarser SR material (Fig. 4a).

Figure 5 shows the θ evolution for the different tested covers at 75 cm depth after the simulation of the extreme rainfall event. The predicted volumetric water content decreased more rapidly for the coarser material (SR material 1 – SM-G), whereas for the finer material (SR material 4 – CL) the predicted volumetric water content decreased much more slowly. At the end of the time period (10 years), the predicted volumetric water content of the coarser and the finer SR materials was respectively 0.05 and 0.13 (similar θ values to those predicted at 100 cm depth).

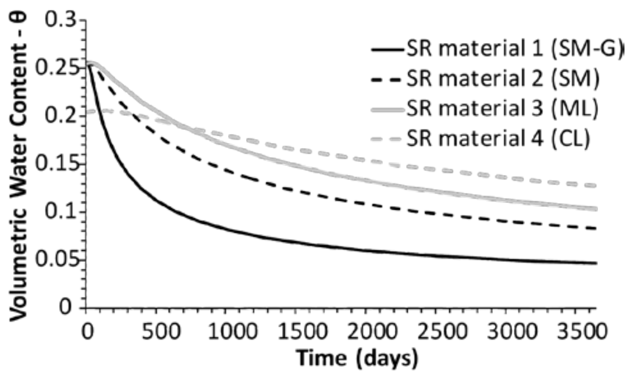

Figure 5. Predicted volumetric water content time trends at 75 cm depth for the four SR materials after the simulation of the PMP value (over ten years)

For these conditions and after the simulation of the extreme rainfall event, Figures 4 and 5 show that the hydrogeological properties of the SR materials affect the distribution of volumetric water contents in time and space. For the finer SR material, the predicted θ values still remained higher than the θ values predicted for the coarser SR material. The difference in volumetric water content calculated at the end of the time period and at depths ranging from 75 to 100 cm was typically 0.08. The SR materials 2, 3 and 4 accumulated water above the interface of the cover systems. The main explanation for this water accumulation is that the natural release capacity of the finer-grained materials is less than the one of the coarser-grained material.

3.2 Release capacity after an extreme rainfall event

As observed in Figures 4a and 5 for the coarser material (SR material 1 – SM-G), water stored after the extreme simulation was rapidly and entirely released to the atmosphere (≈ 512 days after the simulation – Fig. 6a), whereas for the finer material (SR material 4 – CL) only 60% of the net infiltration (*i.e.*, PMP value) was released at the end of the time period (Fig. 6b). For SR materials 2 (SM) and 3 (ML), the water stored in the SR layer was also entirely released about five and eight years after the simulation of the extreme rainfall event (Fig. 6a and 6b). Undeniably, the short-term storage capacity of these materials is more affected than the storage capacity of the coarser SR material. The release rates were approximately 0.30 mm/d for the coarser material (SR material 1 – SM-G), 0.08 and 0.05 mm/d for the SR materials 2 (SM) and 3 (ML), and 0.03 mm/d for the finer material (SR material 4 – CL).

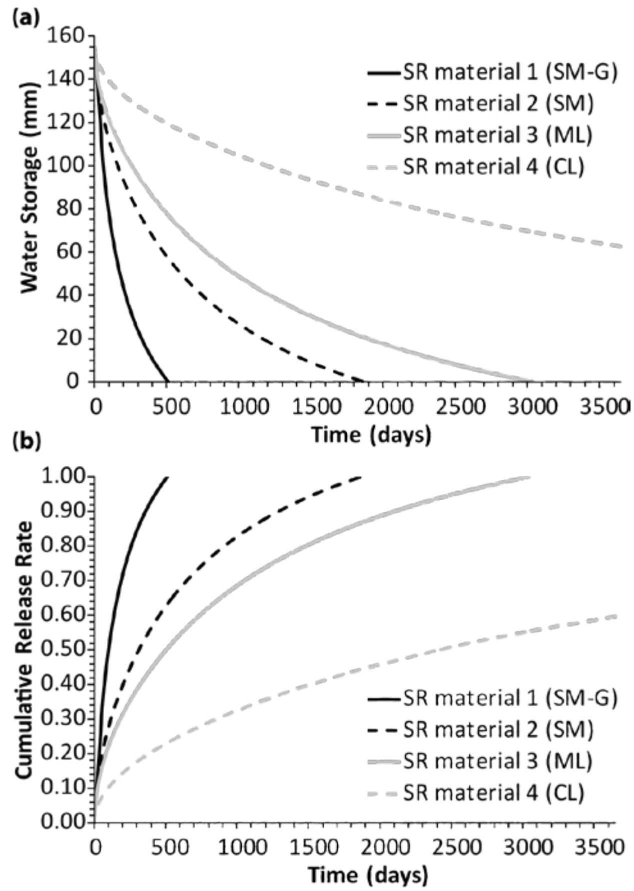

Figure 6. (a) Predicted water storage time trends and (b) cumulative release rate of the extreme rainfall event (155 mm) for the four SR materials

In summary, the hydrogeological properties of the fine-grained materials controlled the release capacity of the SR cover systems. After an extreme rainfall event and due to a lower release capacity, long-term water accumulation occurred for SR cover systems made with the SR materials 2, 3 and 4. This accumulation reduces the storage capacity of the SR cover which could lead to water percolation under consecutive extreme rainfall events.

4 DISCUSSION

Previous results showed that long-term water accumulation can occur above the interface of SR cover systems after an extreme rainfall event. According to Morel-Seytoux (1992), a breakthrough of the capillary break occurs when the SR layer reaches full saturation. In our study, consecutive extreme rainfall events were simulated over ten years to better understand the long-term performance of such cover systems. 155 mm of water was applied the first day of each year for the four cover systems previously simulated. Note that a water column was automatically generated by HYDRUS-1D, with runoff neglected. The initial and boundary conditions were similar to those described in section 2.2.

Figures 7a and 7b show the net infiltration and the water storage time trends for the four SR materials, whereas Figures 8a and 8b present the actual evaporation (*i.e.*, release capacity) and percolation time trends. Table 3 summarizes the predicted water balance components.

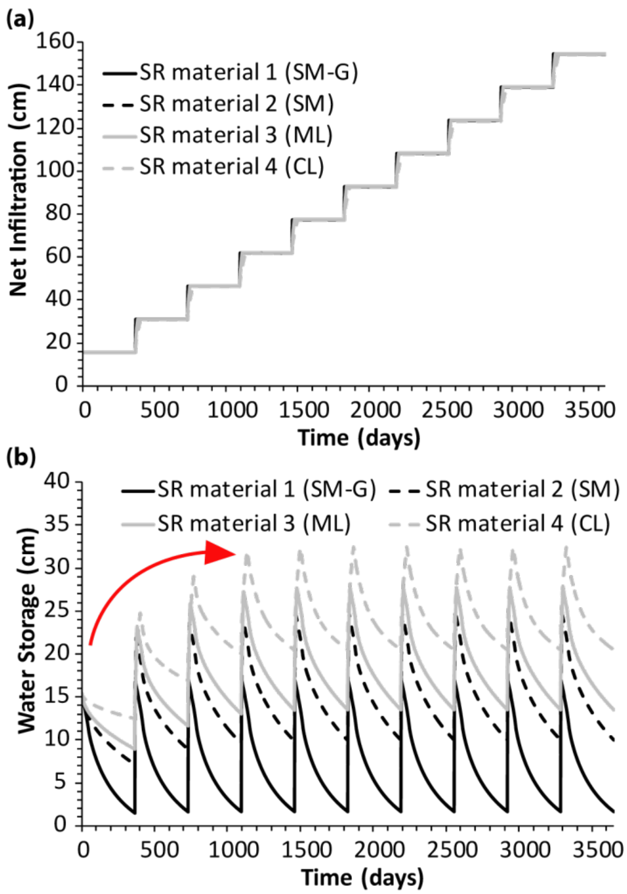

Figure 7. (a) Net infiltration, and (b) water storage time trends during consecutive extreme rainfall events for the four SR materials; the red arrow presents the increase of the water storage during the first extreme rainfall events

Figure 7b shows that the short-term storage capacity of SR materials 2 (SM), 3 (ML) and 4 (CL) is increasingly affected during the first five years where the extreme event is simulated (red arrow). At the end of the time period the water storage reached 10, 14 and 21 cm, respectively, for the three SR materials (Table 3). For the coarser material (SR material 1 – SM-G) the water storage was only slightly affected (2 cm of water storage at the end of the time period; see Table 3). Indeed, after each simulation of the extreme rainfall event, the coarser material (SR material 1 – SM-G) recovered its full storage capacity, whereas for the finer material (SR material 4 – CL) and SR materials 2 (SM) and 3 (ML), water accumulation above the interface of the cover systems increased progressively. Said differently, the system is not able to recover its entire storage capacity between two extreme events.

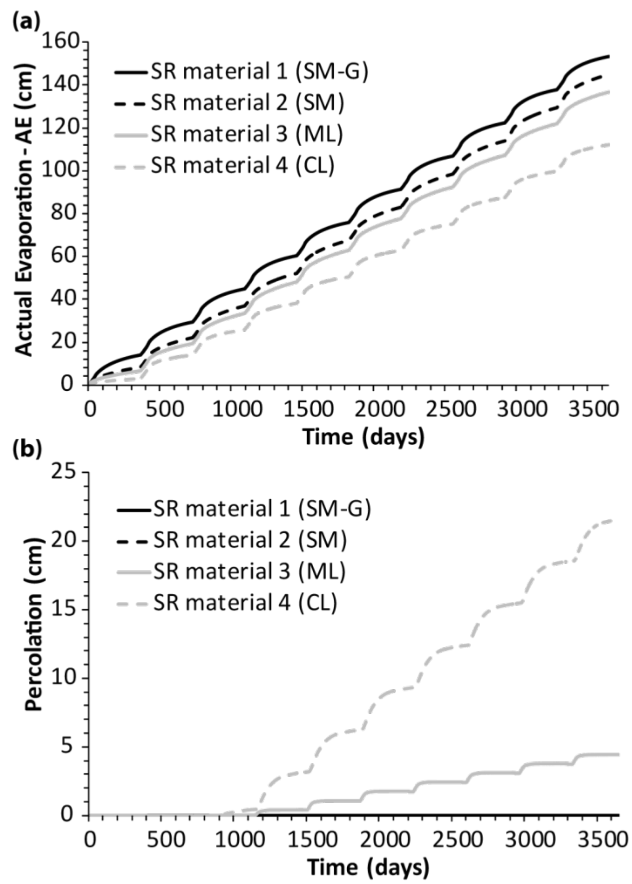

Figure 8. (a) Actual evaporation, and (b) percolation time trends during consecutive extreme rainfall events for the four SR materials

Figure 8a shows that the cumulative actual evaporation of the coarser material (153 cm) was also higher and closer to the net cumulative infiltration (155 cm; see also Table 3). Due to their lower release capacity (*i.e.* actual evaporation; see Fig. 8a), SR materials 3 and 4 accumulated water above the interface of the cover systems and generated water percolation approximately three years after the first simulation (Fig. 8b). At the end of the time period, the predicted water percolation for SR materials 3 and 4 was respectively 4 and 22 mm

(Table 3). Note that although SR material 2 accumulated water at the interface of the cover, no percolation was predicted. Consequently, the natural release capacity of SR materials 1 and 2 validates the long-term performance of these cover systems under consecutive extreme rainfall events.

Table 3. Simulated water balance components (in cm) for consecutive extreme event conditions

Material	Symbol	*Net I*	*S*	*E*	P_r
SR material (1)	**SM-G**	155	2	153	0
SR material (2)	**SM**	155	10	145	0
SR material (3)	**ML**	155	14	137	4
SR material (4)	**CL**	155	21	112	22

Note: *Net I*, net cumulative infiltration; *S*, water storage at end of the modeling; *E*, cumulative actual evaporation; P_r, cumulative percolation (R_0, runoff = 0).

These observations underscore the importance of the hydrogeological properties (more specifically the hydraulic conductivity functions in our study) of fine-grained materials on the long-term performance of SR cover systems under extreme conditions. Due to their higher natural release capacity, the coarser SR materials (*i.e.*, SM-G and SM) recover their full storage capacity more rapidly after consecutive extreme rainfall events, whereas the finer SR materials (*i.e.*, ML and CL) do not prevent water percolation with the reactive mine wastes. Consequently, to design an SR cover system and predict its long-term performance, numerical modeling studies should also investigate the release rate of the SR material under consecutive extreme conditions.

5 CONCLUSIONS

The influence of the hydrogeological properties of fine-grained materials on the release capacity of SR cover systems were numerically investigated under extreme rainfall conditions typical of a semiarid climate. The transient unsaturated water flow of four SR covers made with different fine-grained materials (silty sand with gravel, silty sand, sandy silt and lean clay with sand) was predicted using the HYDRUS-1D code. The main observations are summarized as follows:

- After the simulation of the extreme rainfall event, and although no water percolation was predicted for the four simulations, the coarser SR material (silty sand with gravel) recovered more rapidly its full storage capacity; long-term water accumulation at the bottom interface was predicted for the finer SR materials (sandy silt and lean clay with sand).
- Under consecutive extreme rainfall events, the finer SR materials cannot prevent water percolation due to the increase of the water accumulation at the interface between the SR and CB materials.

These results showed the influence of the fine-grained materials hydrogeological properties on the release capacity of SR cover systems. Coarser SR materials showed a higher release rate than the finer SR materials. Consequently, in the studied case, silty sands would be the most appropriate materials to design SR cover systems and ensure their long-term performance under consecutive extreme rainfall events. In practice, as with storage capacity, the evaluation of the release capacity is important for predicting the long-term performance of SR cover systems.

This study also showed that numerical modeling can be a useful tool to assess hydrogeological behaviour of SR covers submitted to different boundary conditions. Numerical analysis should be used in the design process, in combination with intermediate field scale tests, to evaluate the influence of critical parameters (*e.g.*, the thickness of the SR cover layers, the hydrogeological properties of the cover materials, etc.) on the SR cover performance under natural and extreme climatic conditions.

ACKNOWLEDGEMENTS

Financial support for this study was provided under the International Research Chairs Initiative, a program funded by the International Development Research Centre (IDRC), the Canada Research Chairs Program and the Industrial NSERC Polytechnique-UQAT Chair on Environment and Mines Wastes Management.

REFERENCES

ASTM. 2006. D2434-68: Standard test method for permeability of granular soils, constant head. Annual Book of ASTM Standards, Vol. 04.08.

ASTM. 2009. D 6913-04: Standard test methods for particle-size distribution (gradation) of soils using sieve analysis. Annual Book of ASTM Standards, Vol. 04.09.

ASTM. 2010a. D4318-10: Standard test methods for liquid limit, plastic limit, and plasticity index soils. Annual Book of ASTM Standards, Vol. 04.08.

ASTM. 2010b. D5084-10: Standard test methods for measurements of hydraulic conductivity of saturated porous material using a flexible wall permeameter. Annual Book of ASTM Standards, Vol. 04.08.

ASTM. 2011. D2487: Standard practice for classification of soils for engineering purposes (Unified Soil Classification System). Annual Book of ASTM Standards, Vol. 04.08.

Benson, C.H. 2007. Modeling unsaturated flow and atmospheric interactions. In Theoretical and numerical unsaturated soil mechanics, Schanz T. (ed), Springer Berlin Heidelberg, 113: 187–201.

Bohnhoff, G.L., Ogorzalek, A.S., Benson, C.H., Shackelford, C.D., Apiwantragoon, P. 2009. Field data and water-balance predictions for a monolithic cover in

a semiarid climate. J. Geotech. Geoenv. Eng. 135(3): 333-348.
Bossé, B. 2014. Évaluation du comportement hydrogéologique d'un recouvrement alternatif constitué de rejets calcaires phosphatés en climat semi-aride à aride. Thèse, UQAT, Rouyn-Noranda, Québec, Canada, 331 pp.
Bossé, B., Bussière, B., Hakkou, R., Maqsoud, A., Benzaazoua, M. 2013. Assessment of phosphate limestone wastes as a component of a store-and-release cover in a semiarid climate. Mine Water and the Env. 32(2): 152–167.
Bossé, B., Bussière, B., Hakkou, R., Maqsoud, A., Benzaazoua, M. 2015a. Field experimental cells to assess hydrogeological behaviour of store-and-release covers made with phosphate mine waste. Can. Geotech. J., 52: 1–15.
Bossé, B., Bussière, B., Maqsoud, A., Hakkou, R., Benzaazoua, M. 2015b. Hydrogeological behavior of a store-and-release cover: a comparison between field column tests and numerical predictions with or without hysteresis effects. Mine Water and the Env. (accepted).
Khire, M.V., Benson, C.H., Bosscher, P.J. 2000. Capillary barriers: design variables and water balance. J. Geotech. and Geoenv. Eng. 126(8): 695–708.
Merkus, H.G. 2009. Particle Size Measurements: Fundamentals, Practice, Quality. Springer Particle Technology Series 17. ISBN:978-1-4020-9015-8
Morel-Seytoux, H. 1992. L'effet de barrière capillaire à l'interface de deux couches de sol aux propriétés fort contrastées. Hydrol. Continent. 7(2): 117–128. ISSN:0246-1528
Morris, C.E., Stormont, J.C. 1998. Evaluation of numerical simulations of capillary barrier field tests. Geotech. Geol. Eng. 16(3): 201-213.
Ogorzalek, A.S., Bohnhoff, G.L., Shackelford, C.D., Benson, C.H., Apiwantragroon, P. 2008. Comparison of field data and water-balance predictions for a capillary barrier cover. J. Geotech. Geoenv. Eng. 134(4): 470-486.
Scanlon, B.R., Christman, M., Reedy, R.C., Porro, I., Šimůnek, J., Flerchinger, G.N. 2002. Intercode comparisons for simulating water balance of surficial sediments in semiarid regions. Water Resour. Res. 38(12): 1323–1339.
Šimůnek, J., Šejna, M., Saito, H., Sakai, M., van Genuchten, M.Th. 2009. The HYDRUS-1D software package for simulating the one-dimensional movement of water heat and multiple solutes in variability-saturated media. Dep. of Env. Sci. Univ. of California, Riverside, CA, USA.
Van Genuchten, M.Th. 1980. A closed form equation for predicting the hydraulic conductivity of unsaturated soils. Soil Sci. Soc. Am. J. 44: 892-898.
Zhan, G., Keller, J., Milczarek, M., Giraudo, J. 2014. 11 Years of Evapotranspiration Cover Performance at the AA Leach Pad at Barrick Goldstrike Mines. Mine Water and the Env, 33(3): 195–205.